Applied Surface Science 255 (2009) 5003–5008

Contents lists available at ScienceDirect

Applied Surface Science

journal homepage: www.elsevier.com/locate/apsusc

Integration and characterization of aligned carbon nanotubes on metal/silicon substrates and effects of water

Yong Zhang [a], Ruying Li [a], Hao Liu [a], Xueliang Sun [a,*], Philippe Mérel [b], Sylvain Désilets [b]

[a] Department of Mechanical and Materials Engineering, University of Western Ontario, London, ON. N6A 5B9, Canada
[b] Defence Research & Development Canada- Valcartier, 2459 Boulevard Pie-XI nord, Québec, QC G3J 1X5, Canada

ARTICLE INFO

Article history:
Received 10 July 2008
Received in revised form 27 October 2008
Accepted 21 December 2008
Available online 27 December 2008

PACS:
61.48.De
81.07.De
81.07.Lk
81.15.Gh

Keywords:
Carbon nanotubes
Chemical vapor deposition
Metal/Silicon substrate
Water vapor

ABSTRACT

We report here a facile way to grow aligned multi-walled carbon nanotubes (MWCNTs) on various metal (e.g. gold, tungsten, vanadium and copper)/silicon electrically conductive substrates by aerosol-assisted chemical vapor deposition (AACVD). Without using any buffer layers, integration of high quality MWCNTs to the conductive substrates has been achieved by introducing appropriate amount of water vapor into the growth system. Scanning electron microscopy (SEM) and transmission electron microscopy (TEM) determination indicate tidy morphology and narrow diameter distribution of the nanotubes as well as promising growth rate suitable for industrial applications. Raman spectra analysis illustrates that the structural order and purity of the nanotubes are significantly improved in the presence of water vapor. The growth mechanism of the nanotubes has been discussed. It is believed that water vapor plays a key role in the catalyst-substrate interaction and nucleation of the carbon nanotubes on the conductive substrates. This synthesis approach is expected to be extended to other catalyst-conductive substrate systems and provide some new insight in the direct integration of carbon nanotubes onto conductive substrates, which promises great potential for applications in electrical interconnects, contacts for field emitters, and other electronic nanodevices.

1. Introduction

As one of the most promising candidates to replace the role of conventional building blocks in various fields ranging from electronics to biotechnology, carbon nanotubes (CNTs) have received wide-spread attention in terms of both fundamentals and practical applications [1]. Indeed, numerous nano-scale electronic devices based on CNTs such as various transistors [2–6], sensors [7], super-capacitors [8], thermal rectifiers [9], and resistors [10] have been successfully achieved. Among various CNT synthesis approaches, chemical vapor deposition allows direct growth of CNTs on substrates with selective large area and vertical alignment. Compared to conventional thermal chemical vapor deposition, aerosol-assisted chemical vapor deposition has attracted more attention for synthesizing CNTs due to its versatility and quality of CNTs obtained [11,12]. Thus it has been considered a preferred CNT growth method for nanodevice applications.

In order to build various nanodevices, controlled growth of CNTs on suitable substrates is clearly one of the key issues. For most practical applications, high quality contact between carbon nanotubes and conductive substrates (e.g. metallic or metal-coated silicon substrates) is essential to provide *in situ* electrical end-connection for the individual CNTs [13], and to avoid potential defects as well as contamination arising from processing conditions [14,15]. Unfortunately, the growth of CNTs on metal substrates suffers from poor availability of catalysts induced by a strong catalyst-substrate interaction, which has confined the growth of CNTs mainly on non-conductive substrates and inevitably restricted their applications [13]. According to a report by Cao et al., for example, a gold layer on quartz substrate would heavily suppress the growth of CNTs and could act as the template to pattern the growth of CNTs [16]. Recently, effect of metallic substrate on CNTs growth has been investigated and some beneficial techniques have been developed to circumvent this limitation. Ng et al. attempted several catalyst–metal-layer combinations and obtained aligned CNTs on the combination of Ni and FeNi catalyst/Al buffer layer [17]. Wang et al. achieved patterned CNTs on some metal or metal-coated substrates using a floating method; however, it was not suitable for gold and copper substrates [18]. Matthews et al. employed Al/Fe thin films as catalysts and generated CNTs with random orientation on gold and molybdenum substrates [19]. Talapatra et al. achieved aligned

* Corresponding author. Tel.: +1 519 661 2111x87759; fax: +1 519 661 3020.
E-mail address: xsun@eng.uwo.ca (X. Sun).

0169-4332/$ – see front matter © 2008 Elsevier B.V. All rights reserved.
doi:10.1016/j.apsusc.2008.12.053

CNTs on an Inconel substrate using the floating-catalyst CVD method, which is not applicable to gold, silicon and copper [20]. More recently, Parthangal et al. successfully achieved the growth of CNTs onto several metal and alloy substrates by employing a bimetallic iron/alumina (Fe/Al_2O_3) composite catalyst [21]. Nevertheless, a catalyst-covered substrate or alumina buffer layer is generally used to ensure CNTs growth on various metal substrates.

Recently, the introduction of water vapor into the process of synthesizing CNTs has proved to be an effective technique to purify and promote growth of CNTs. It has been proposed that water can enhance the activity and lifetime of catalysts by removing carbonaceous impurities [22–27]. Considering the challenge of growing CNTs on different bulk metals, it may be an alternative approach to synthesize CNTs on various metal-coated silicon substrates, which not only ensures the superior electrical conductivity of the substrate as a current collector, but also enhances the incorporation of CNTs functionality with the Si electronics. However, the effects of water on the growth of CNTs on various metallic/silicon substrates using the AACVD method have not been studied.

In this paper, we demonstrate the growth of CNTs on various metal-coated silicon substrates by using a water-assisted AACVD method with emphasis on effects of water. The results show that the introduction of water vapor not only ensures the growth of CNTs on the conductive substrate, but also significantly improves the growth quality of the CNTs, including much higher growth rate, fewer impurities and better vertical alignment.

2. Experimental details

To obtain various metal-coated silicon substrates, some commonly-used metal (Au, W, V and Cu) layers with the thickness of 1 μm were deposited directly on silicon substrate by radio frequency (RF) magnetron sputtering using corresponding metal targets (purity 99.99%) with high purity argon (purity 99.999%). The sputtering was carried out under the pressure of 4.6×10^{-3} Torr and a power of 300 W. The AACVD method used for nanotube growth is based on the catalytic decomposition of liquid hydrocarbons from the pyrolysis of mixed aerosols containing both the hydrocarbon and the metallic source. The pyrolitic mixture is carried to the reactor simultaneously and continuously [28]. In the hot zone, the solvent evaporates and ferrocene decomposes to provide the iron catalyst required for nanotube growth. In our experiments, the synthesis of MWCNTs was carried out by an AACVD system shown in Fig. 1. The system is basically composed of three different parts: an aerosol generator (Type 7901, RBI, France), a modified quartz chamber placed in a furnace (Linderberg/Blue M) and a gas trap for the exhausting gases. There

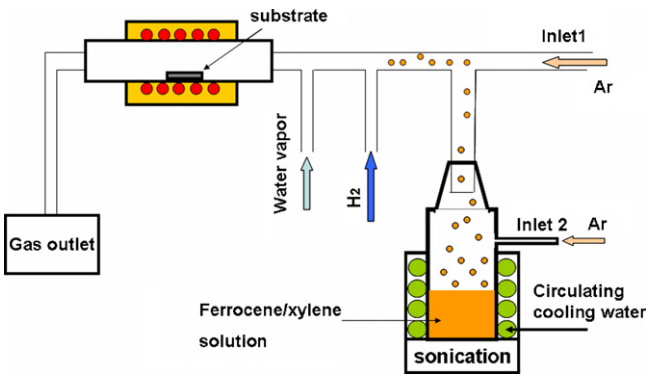

Fig. 1. Schematic diagram of aerosol-assisted chemical vapor deposition system for growing carbon nanotubes.

are two argon inlets in this system. Inlet 1 is used for purging the system and to dilute aerosol concentration. Inlet 2 is used to carry the aerosol. Ferrocene acts as the catalyst precursor and m-xylene is the carbon feedstock. The typical CNTs carpet is obtained from pyrolysis of a 5 wt% ferrocene solution dissolved in m-xylene. The aerosol is produced by sonication. First, various substrates were put inside the chamber. Secondly, an argon flow of 400 sccm was passed through the reactor to purge the system for 20 min. Thirdly, the furnace was heated to 850 °C within 15 min. As soon as the temperature reached 850 °C, the aerosol droplets were produced by ultrasonication with a frequency of 850 kHz and transported by argon gas introduced from Inlet 2 at a flow rate of 1000 sccm, while the flow rate of argon in Inlet 1 was increased from 400 to 600 sccm to dilute the generated aerosol. At the same time, hydrogen was introduced with a flow rate of 1000 sccm as the reaction gas. Water vapors were carried into the reactor with flowing argon (10 sccm) through a water bubbler during the growth period (Fig. 1). The growth time was 25 min. At the end of the experiment, the aerosol generator and furnace were turned off and argon flow in Inlet 2 was also stopped. argon continued to flow in Inlet 1, and hydrogen and water vapor were kept passing through the reactor until the furnace cooled down to room temperature. All our experiments were performed at atmospheric pressure. The morphology and structure of CNTs were characterized using a Hitachi S-4500 field-emission scanning electron microscope (FESEM) operated at 5.0 kV, JEOL 2010F transmission electron microscope (TEM) operated at 200 kV and Raman analysis which was performed on a Horiba Jobin Yvon high resolution (HR800) confocal spectrometer operating with an incident laser beam at 632.8 nm.

3. Results and discussion

Fig. 2(a–d) shows SEM images of the CNTs grown on a gold/silicon substrate without and with the introduction of water vapor, respectively. In the absence of water vapor, the low magnification SEM image in Fig. 2(a) shows that the irregularly twisted CNTs were obtained with the length of around 150 μm. An increased magnification of the SEM image in Fig. 2(b) reveals numerous particles attached on the outer surface of the CNTs. When the water vapor was introduced, vertically aligned CNTs were obtained. Further, the length of the CNTs obtained was 450 μm for the same period of growth time, indicating significant increase of growth rate, as shown in Fig. 2(c). A closer inspection of the CNTs reveals that the CNTs are uniform and smooth with few impurity particles (Fig. 2(d)).

Fig. 3 shows SEM images of the CNTs grown on a tungsten/silicon substrate without and with the introduction of water vapor, respectively. In the absence of water vapor, only random, sparse CNTs were obtained with a length of around 10 μm, as shown in Fig. 3(a) and (b). In the presence of water vapor, aligned CNTs were achieved with a length over 90 μm (Fig. 3(c)), indicating a dramatic improvement in the morphology and growth rate. From the increased magnification image in Fig. 2(d), random lateral growth of bundles of aligned CNTs can be observed and the diameter of the CNTs is between 30–60 nm.

Fig. 4 shows SEM images of the CNTs grown on a vanadium/silicon substrate without and with the introduction of water vapor, respectively. While no water vapor was introduced, no obviously discernable CNTs were collected on the substrate and only some fiber-like 1D nanostructures were generated as shown in Fig. 4(a) and (b). By introducing water vapor, the growth of aligned CNTs was observed as shown in Fig. 4(c) and (d). Compared to the cases of Au/Si and W/Si substrates, the length of the CNTs is shorter, about 25 μm. In this case, diameter of the nanotube is quite uniform and is larger with typical diameters of 80–110 nm.

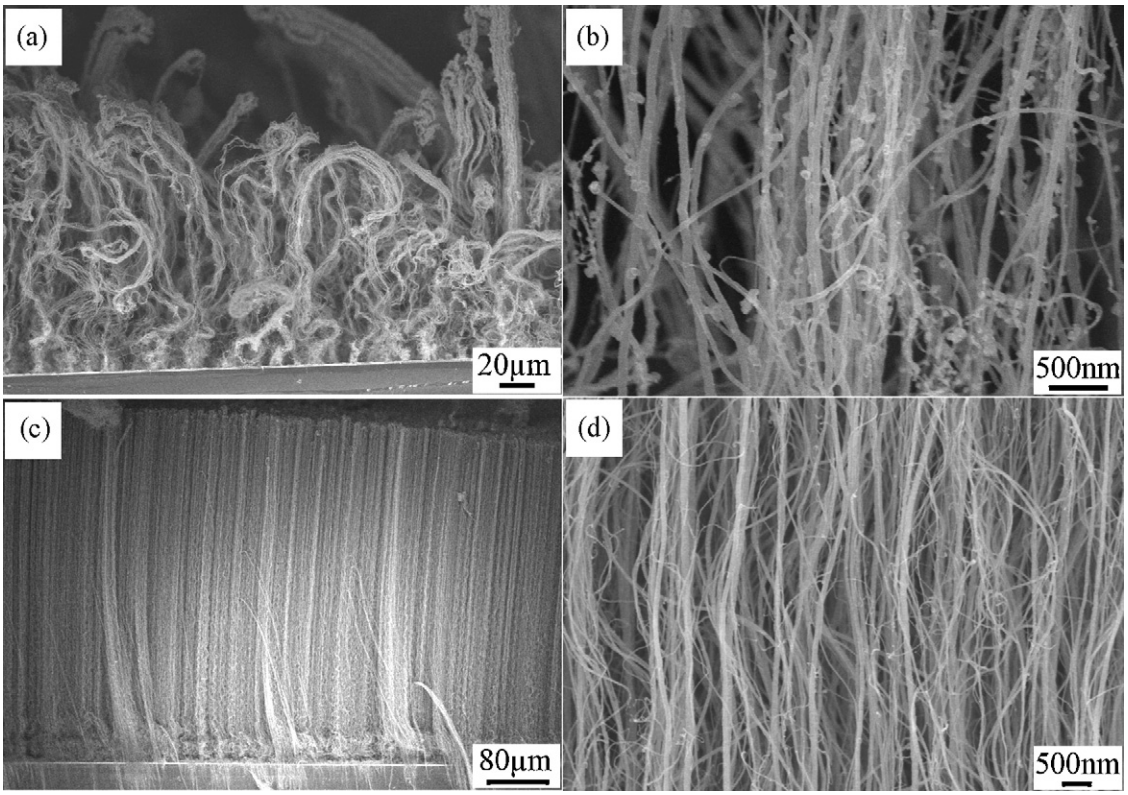

Fig. 2. SEM images of carbon nanotubes grown on Au/Si substrate without (a, b), and with (c, d) water vapor.

In the case of copper substrate, no CNTs growth occurred in the absence of the water vapor. As the water vapor was introduced, randomly oriented noodle-like bundles of CNTs were observed (Fig. 5(a)). The increased magnification SEM image shows that the noodle-like bundles consist of very uniform CNTs (Fig. 5(b)).

In order to understand and compare effects of water on MWCNTs growth on the four substrates, detailed growth characterizations

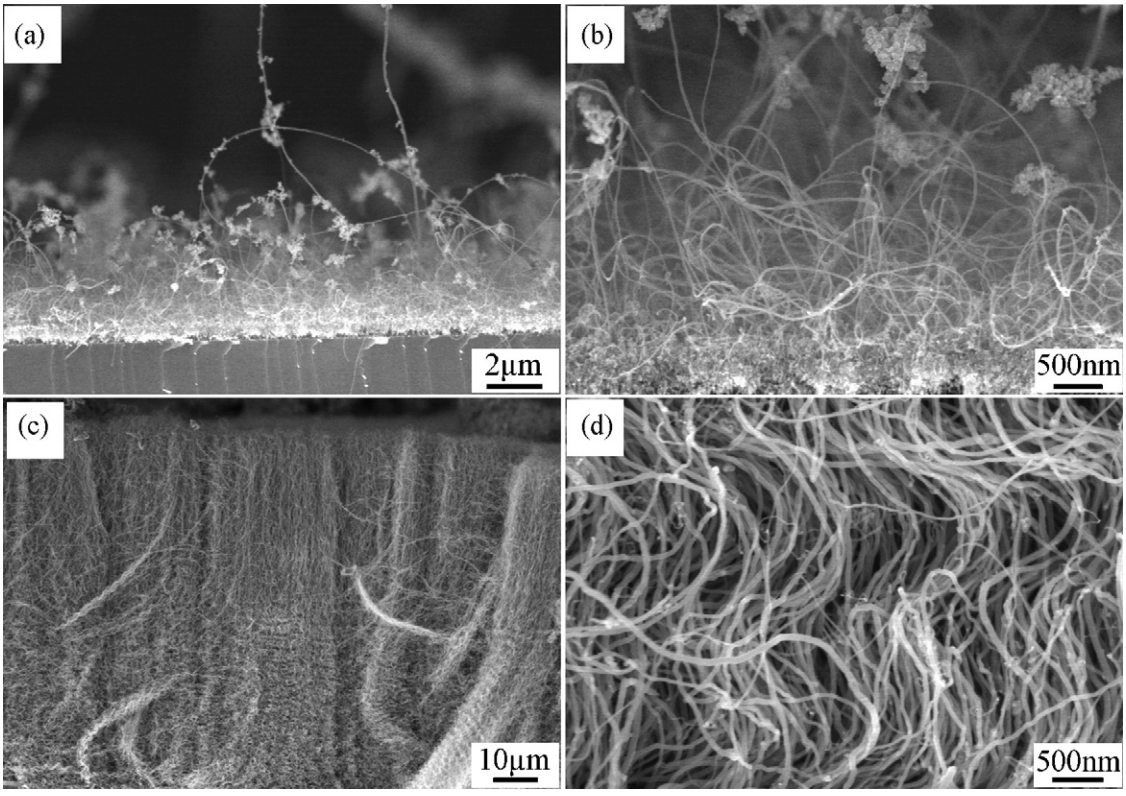

Fig. 3. SEM images of carbon nanotubes grown on W/Si substrate (a, b) without, and with(c, d) water vapor.

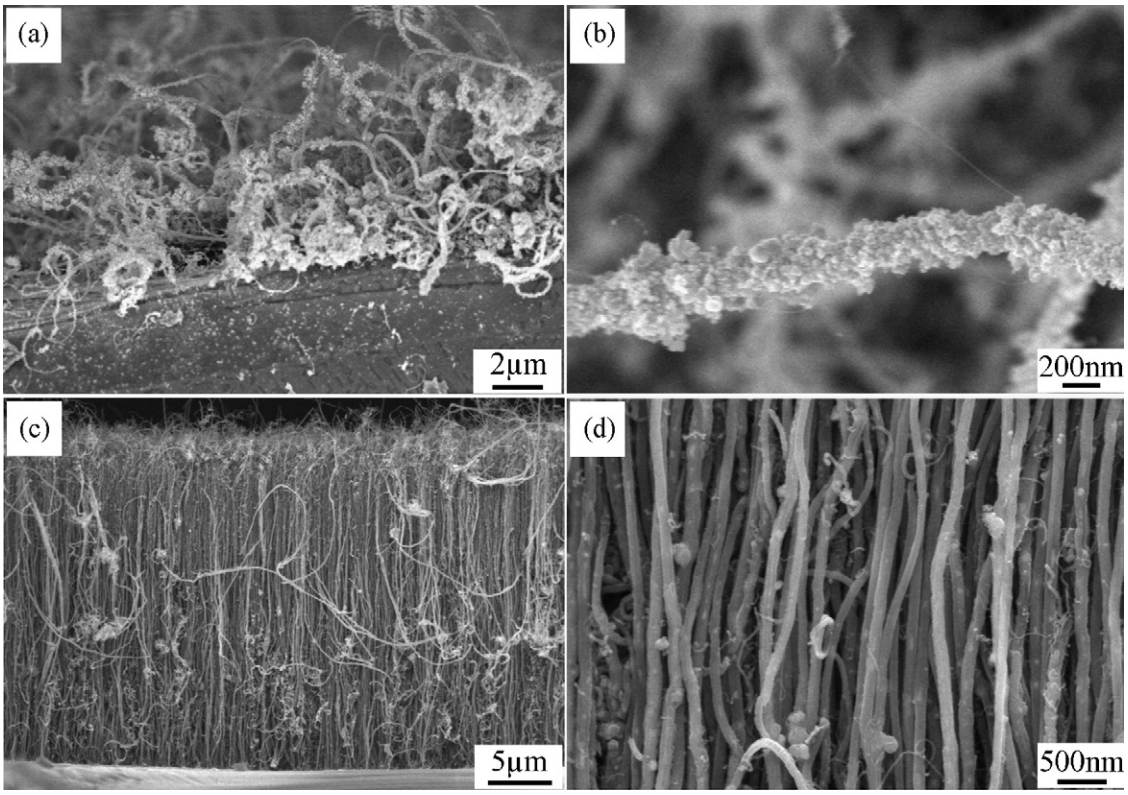

Fig. 4. SEM images of carbon nanotubes grown on V/Si substrate (a, b) without, and (c, d) with water vapor.

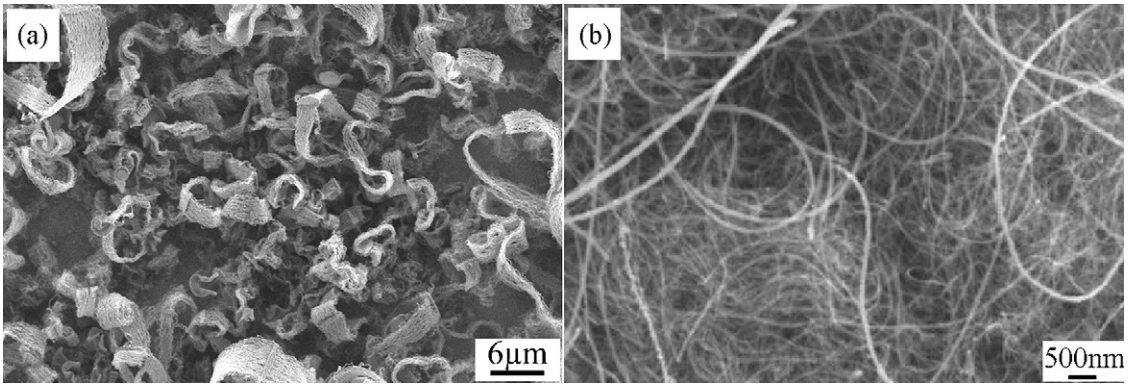

Fig. 5. SEM images of carbon nanotubes grown on Cu/Si substrate with water vapor.

including growth rate, orientation degree and morphology are summarized in Table 1. Obviously, the introduction of the water vapor promoted the growth rate of CNTs and resulted in narrow distribution of the nanotube diameter and improved the quality of CNTs by removing impurities attached on the CNTs. In the absence of water vapor, only gold/silicon and tungsten/silicon substrates led to CNT growth, but with poor quality. In the presence of water vapor, it was possible to grow CNTs on the four types of substrate. In addition, the growth rate and quality of the nanotubes were significantly improved on the gold/silicon and tungsten/silicon substrates.

In order to further characterize the structure and morphology of CNTs, TEM observations were carried out on the CNTs obtained

Table 1
Growth comparison of the CNTs grown on different metal/Si substrates.

Substrate	Growth rate (μm/min)		Orientation		Morphology	
	NWA	WA	NWA	WA	NWA	WA
Au/Si	6	18	Aligned	Well aligned	Not clean	Very clean
W/Si	0.3–0.5	3–4	Random	Well aligned	Not clean	Very clean
V/Si	–	1	–	Aligned	–	Clean
Cu/Si	–	1.5–2	–	Random	–	Not clean

NWA: Non water-assisted growth WA: Water-assisted growth.

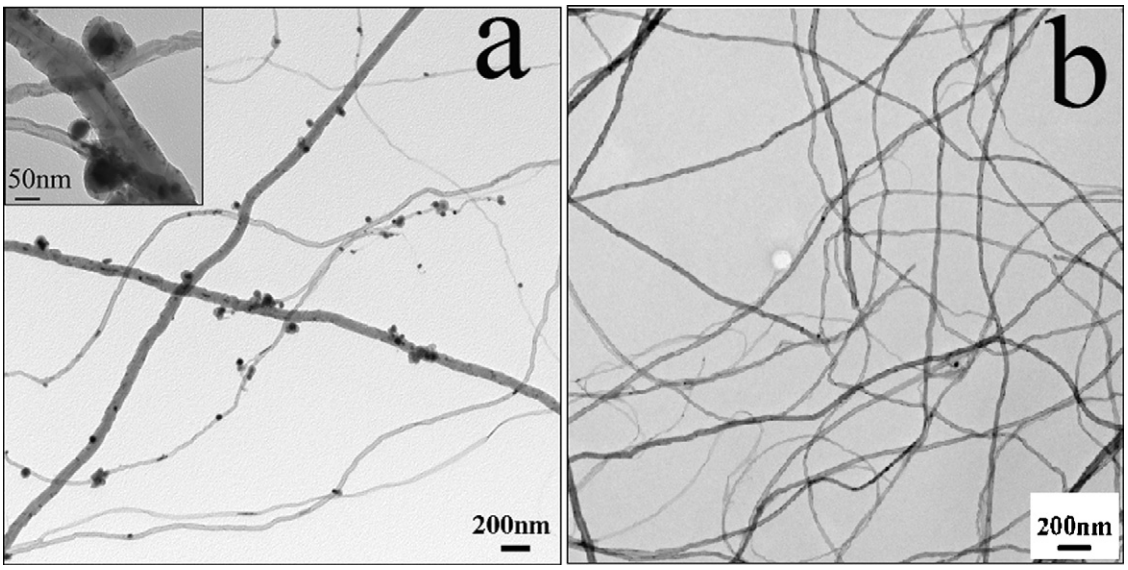

Fig. 6. TEM images of the carbon nanotubes grown on gold/Si substrate (a) without and (b) with water vapor. Inset image in Fig. 6(a): magnified image of the nanoparticles attached on the nanotubes.

with and without water vapor. Because it is difficult to harvest CNTs from the tungsten/silicon and vanadium/silicon substrates in the cases grown in the absence of water vapor, the CNTs grown on the gold/silicon substrate were collected for TEM experiments. Fig. 6 shows TEM images of the CNTs on gold/silicon obtained without and with water vapor. In the absence of water vapor, the nanotubes are highly non-uniform with the diameter ranging from 20–100 nm and numerous nanoparticles are embedded on the nanotube surface (Fig. 6(a)). The increased magnification image of the particles attached on the nanotubes is displayed in the inset image in Fig. 6(a), showing that the Fe catalyst nanoparticles are coated with a layer of carbon. In the case of the water vapor based synthesis, tidy CNTs with uniform diameter are obtained (Fig. 6(b)). Further, the outer diameter is around 40 nm and the wall thickness is around 8 nm, and the inner diameter is around 24 nm. General observations on the CNTs in different regions reveal that the water-assisted CNTs possess thinner walls than the CNTs synthesized without water vapor, while the inner diameter of the nanotubes remains constant.

Fig. 7(a) and (b) show the typical Raman spectra of the MWCNT grown on a gold/silicon substrate before and after introducing water vapor, respectively. D and G bands dominate the first-order region. G′ arising from double resonance processes is observed in the second-order region of the spectra [29]. The shape and intensity ratio evolution of D, G, and G′ bands reflect the changes in crystalline perfection and phase purity produced by the variation of the growth conditions [30]. The D/G band intensity ratio (I_D/I_G) is commonly reported to increase with increasing defects in graphene layers and structural disorder originating from the amorphous carbon inclusions, while G′/G intensity ratio ($I_{G'}/I_G$) is evaluated monitoring the smoothness-degree of graphene sheets. [31]. By introducing water vapor, I_D/I_G decreases from 0.71 to 0.66, while $I_{G'}/I_G$ increases from 0.42 to 0.58 (Fig. 7(a) and (b)). Therefore, we can conclude that the introduction of appropriate amount of water vapor improves the structural order and purity of the MWCNT sample.

For CNTs growth by the AACVD method, ferrocene is dissolved in m-xylene and acts as the catalyst precursor. At high temperature, the solvent evaporates and ferrocene decomposes to provide iron particles. The iron particles are deposited onto substrates and act as active nucleation centers for nanotube growth. Although the precise role of the water vapor is not clear at present, we think that the effects of the water vapor are displayed in two aspects: one is the influence of water on the catalyst particles and the other is the influence of water on the substrates.

In the first effect, iron oxide nanoparticles are supposed to be formed due to oxidation of iron particles under high temperature in a moist atmosphere, which not only avoids the diffusion of iron atoms into the metal substrate [32], but also strengthens the

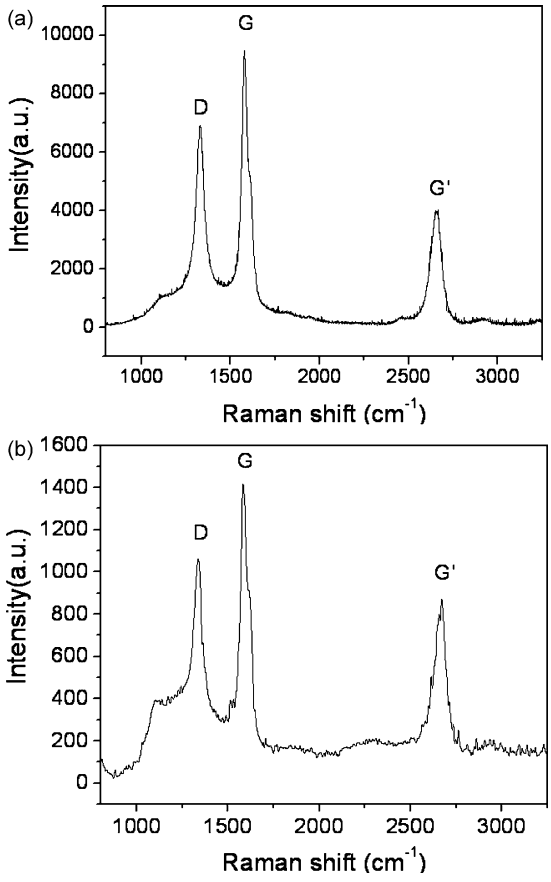

Fig. 7. Raman spectra of the carbon nanotubes grown on gold/Si substrate (a) without and (b) with water vapor.

adhesion between the catalyst particles and the metal substrates, and favors the formation of high-density catalyst nanoparticles for CNTs growth. In addition, water vapor acts as a weak oxidizer that can remove the amorphous carbon on the catalyst surface and enhance the activity and lifetime of the catalyst [24], which significantly increases the growth rate and length of the CNTs. At the same time, water vapor removes the carbonaceous impurities from the CNTs and catalyst particles, with fresh surface further strengthening oxidation of carbon, which results in the growth of CNTs with clean morphology and thinner walls [27].

In the second effect, it has been known that strong catalyst-metal substrate interaction prevents CNTs from growing due to the high surface tension of non-catalytic metals [33]. On the other hand, minimal surface diffusion of the catalyst particles favors nucleation of CNTs. The introduction of an appropriate amount of water vapor may modify the surface of the metal and balance these factors to facilitate generation of active catalyst particles and promote CNTs growth. It should be noted that influence of water vapor may differ for different metals, which would explain the observation that CNTs growth on the four metal-coated silicon substrates displayed different performances.

4. Conclusion

We have developed a simple procedure to grow CNTs in a controlled way on Au, W, V and Cu coated silicon substrates by using aerosol-assisted chemical vapor deposition in the presence of water vapor. Vertically aligned CNTs with uniform diameter, elevated growth rates and neat morphologies can be achieved on the substrates. The water vapor is thought to play a key role in balancing the effect of the catalyst-substrate interaction and nucleation of the CNTs on the conductive substrates. Integration of the CNTs on the conductive substrates has great potential applications for field emitters as well as other electrical interconnect applications.

Acknowledgement

This research was supported by Department of National Defence, Natural Sciences and Engineering Research Council of Canada (NSERC), NSERC Canada Research Chair (CRC) Program, Canada Foundation for Innovation (CFI), Ontario Research Fund (ORF), Ontario Early Researcher Award (ERA) and the University of Western Ontario.

References

[1] R.H. Baughman, A.A. Zakhidov, W.A. de Heer, Science 297 (2002) 787.
[2] A. Bachtold, P. Hadley, T. Nakanishi, C. Dekker, Science 294 (2001) 1317.
[3] A. Javey, J. Guo, Q. Wang, M. Lundstrom, H.J. Dai, Nature 424 (2003) 654.
[4] K. Keren, R.S. Berman, E. Buchstab, U. Sivan, E. Braun, Science 302 (2003) 1380.
[5] A. Javey, J. Guo, D.B. Farmer, Q. Wang, E. Yenilmez, R.G. Gordon, M. Lundstrom, H.J. Dai, Nano Lett. 4 (2004) 1319.
[6] P.J. Herrero, J.A. van Dam, L.P. Kouwenhoven, Nature 439 (2006) 953.
[7] A. Modi, N. Koratkar, E. Lass, B.Q. Wei, P.M. Ajayan, Nature 424 (2003) 171.
[8] D.N. Futaba, K. Hata, T. Yamada, T. Hiraoka, Y. Hayamizu, Y. Kakudate, O. Tanaike, H. Hatori, M. Yumura, S. Iijima, Nat. Mater. 5 (2006) 987.
[9] C.W. Chang, D. Okawa, A. Majumdar, A. Zettl, Science 314 (2006) 1121.
[10] S. Frank, P. Poncharal, Z.L. Wang, W.A. de Heer, Science 280 (1998) 1744.
[11] M. Pinault, M. Mayne-L'Hermite, C. Reynaud, O. Beyssac, J.N. Rouzaud, C. Clinard, Diamond Relat. Mater. 13 (2004) 1266.
[12] S.R.C. Vivekchand, L.M. Cele, F.L. Deepark, A.R. Raju, A. Govindaraj, Chem. Phys. Lett. 386 (2004) 313.
[13] S. Talapatra, S. Kar, S.K. Pal, R. Vajtai, L. CI, P. Victor, M.M. Shaijumon, S. Kaur, O. Nalamasu, P.M. Ajayan, Nat. Nanotechnol. 1 (2006) 112.
[14] N.R. Franklin, Q. Wang, T.W. Tombler, A. Javey, M. Shim, H.J. Dai, Appl. Phys. Lett. 81 (2002) 913.
[15] T.K. Kim, J.M. Zuo, E.A. Olsen, I. Petrov, Appl. Phys. Lett. 87 (2005) 173108.
[16] A.Y. Cao, X.F. Zhang, C.L. Xu, J. Liang, D.H. Wu, B.Q. Wei, Appl. Surf. Sci. 181 (2001) 234.
[17] H.T. Ng, B. Chen, J.E. Koehne, A.M. Cassell, J. Li, J. Han, M. Meyyappan, J. Phys. Chem. B 107 (2003) 8484.
[18] B. Wang, X. Liu, H. Liu, D. Wu, H. Wang, J. Jiang, X. Wang, P. Hu, Y. Liu, D. Zhu, J. Mater. Chem. 13 (2003) 1124.
[19] K.D. Matthews, M.G. Lemaitre, T. Kim, H. Chen, M. Shim, J.M. Zuo, J. Appl. Phys. 100 (2006) 044309.
[20] S. Talapatra, S. Kar, S.K. Pal, R. Vajtai, L. Ci, P. Victor, M.M. Shaijumon, S. Kaur, O. Nalamasu, P.M. Ajayan, Nat. Nanotechnol. 1 (2006) 112.
[21] P.M. Parthangal, R.E. Cavicchi, M.R. Zachariah, Nanotechnology 18 (2007) 185605.
[22] K. Tohji, T. Goto, H. Takahashi, Y. Shinoda, N. Shimizu, B. Jeyadevan, I. Matsuoka, Nature 383 (1996) 679.
[23] J.M.C. Moreno, M. Yoshimura, J. Am. Chem. Soc. 123 (2001) 741.
[24] K. Hata, D.N. Futaba, K. Mizuno, T. Namai, M. Yumura, S. Iijima, Science 306 (2004) 1362.
[25] Z.H. Kang, E.B. Wang, L. Gao, S.Y. Lian, M. Jiang, C.W. Hu, L. Xu, J. Am. Chem. Soc. 125 (2003) 13652.
[26] G. Tobias, L.D. Shao, C.G. Salzmann, Y. Huh, M.L.H. Green, J. Phys. Chem. B 110 (2006) 22318.
[27] Z.B. Zhao, J.Y. Qu, J.S. Qiu, X.Z. Wang, Z.Y. Wang, Chem. Commun. (2006) 594.
[28] X.H. Hou, K.L. Choy, Chem. Vap. Deposition 12 (2006) 583.
[29] M.S. Dresselhaus, G. Dresselhaus, R. Saito, A. Jorio, Phys. Rep. 409 (2005) 47.
[30] R.A. DiLeo, B.J. Landi, R.P. Raffaelle, J. Appl. Phys. 101 (2007) 064307.
[31] M.G. Donato, G. Messina, S. Santangelo, S. Galvagno, C. Milone, A. Pistone, J. Phys.: Conf. Ser. 61 (2007) 931.
[32] M.S. Kabir, R.E. Morjan, O.A. Nerushev, P. Lundgren, S. Bengtsson, P. Enokson, E.E.B. Campbell, Nanotechnology 16 (2005) 458.
[33] T. Katayama, H. Araki, H. Kajii, K. Yoshino, Synth. Met. 121 (2001) 1235.